

- Tsai, M.-D., Jiang, R.-T., & Bruzik, K. (1983) *J. Am. Chem. Soc.* 105, 2478-2480.
- Van Dijck, P. W. M., DeKruijff, B., Aarts, P. A. M. M., Verkleij, A. J., & DeGier, J. (1978) *Biochim. Biophys. Acta* 506, 183-191.
- Vasilenko, I., DeKruijff, B., & Verkleij, A. J. (1982) *Biochim. Biophys. Acta* 685, 144-152.
- Vaughan, D. J., & Keough, K. M. (1974) *FEBS Lett.* 47, 158-161.
- Viti, V., & Minetti, M. (1981) *Chem. Phys. Lipids* 28, 215-225.
- Yeagle, P. L. (1978) *Acc. Chem. Res.* 11, 321-327.
- Yeagle, P. L., Hutton, W. C., Huang, C.-H., & Martin, R. B. (1975) *Proc. Natl. Acad. Sci. U.S.A.* 72, 3477-3481.
- Yeagle, P. L., Hutton, W. C., Huang, C.-H., & Martin, R. B. (1976a) *Biochemistry* 15, 2121-2124.
- Yeagle, P. L., Hutton, W. C., Martin, R. B., Sears, B., & Huang, C.-H. (1976b) *J. Biol. Chem.* 251, 2110-2112.

## Acyl Chain Interdigitation in Saturated Mixed-Chain Phosphatidylcholine Bilayer Dispersions<sup>†</sup>

S. W. Hui,\* J. T. Mason, and Ching-hsien Huang\*

**ABSTRACT:** The molecular packing of various fully hydrated mixed-chain phosphatidylcholines was studied by X-ray diffraction and electron microscopy. All of the mixed-chain phosphatidylcholines under study were shown to adopt a lamellar or bilayer form in aqueous media. The bilayer thickness of these mixed-chain phosphatidylcholines was determined from the lamellar repeat distance in the small-angle X-ray diffraction region by controlled swelling experiments. At  $T > T_m$ , the bilayer thickness of C(18):C(12)PC and C(18):C(10)PC is found to be comparable to that of C(14):C(14)PC. In contrast, the bilayer thickness of these highly asymmetric phosphatidylcholines is considerably less than that of the symmetric C(14):C(14)PC at temperatures below  $T_m$ . Moreover, the wide-angle X-ray diffraction patterns taken at  $T < T_m$  consist of at least two sharp reflections at 4.2 and 4.6 Å. These X-ray diffraction data suggest that these highly asymmetric mixed-chain phospholipids, in excess water, form mixed interdigitated bilayers in the gel state and that the acyl chain packing in the gel-state bilayer is not hexagonal. The freeze-fracture planes of these mixed-chain phosphatidyl-

cholines are discontinuous at  $T < T_m$ , supporting the conclusion drawn from X-ray diffraction data that these highly asymmetric phosphatidylcholines form interdigitated bilayers at temperatures below  $T_m$ . The molecular packing of fully hydrated C(18):C(14)PCs in bilayers is distinctively different from that of C(18):C(10)PCs or C(18):C(12)PCs. On the basis of swelling experiments, the bilayer thickness of C(18):C(14)PC lamellae at temperatures below  $T_m$  is found to be significantly larger than that of C(18):C(10)PCs but slightly less than that of C(14):C(14)PCs at the same reduced temperature. These data are taken as strong evidence to argue in favor that the asymmetric acyl chains of C(18):C(14)PCs do not adopt an interdigitated conformation as proposed for C(18):C(10)PCs in the gel state. Freeze-fracture electron micrographs are also presented to show that large C(18):C(14)PC structures undergo gross morphological changes as the phospholipid-H<sub>2</sub>O system is heated through the pretransition and main transition temperatures. The significance and implication of our studies on these mixed-chain phosphatidylcholines in biomembranes are discussed.

**A**symmetric synthetic phospholipids in which the two acyl chains are different in carbon number provide a convenient means to study the molecular packing of mixed-chain phospholipids in bilayer membranes. Because of an abrupt *sn*-2 chain bend at the C(2) atom near the glycerol backbone region (Pearson & Pascher, 1979), there is a mismatch in the packing of the terminal methyl ends of the two phosphatidylcholine acyl chains in the gel-state bilayer even if the bilayer is composed of symmetric phospholipids in which both the *sn*-1 and *sn*-2 acyl chains are of equal carbon numbers (Mason & Huang, 1981; Huang & Levin, 1983). This mismatching is further exaggerated if the *sn*-1 acyl chain has more methylene units than the *sn*-2 acyl chain. It has been suggested that asymmetric phosphatidylcholines in which the *sn*-1 acyl chain is longer than the *sn*-2 chain by more than four methylene units

would form an interdigitated bilayer in the gel state (Mason et al., 1981; Huang et al., 1983). The mismatching and interdigitation have been suggested to affect both the inter- and intrachain order/disorder processes in bilayers (Huang et al., 1982, 1983) and the vesicle size of lipid dispersions (Mason et al., 1983).

Recently, acyl chain interdigitation in fully hydrated phospholipid bilayers has been suggested by Ranck et al. (1977) and Ranck & Tocanne (1982) for dipalmitoylphosphatidylglycerol bilayers, based on X-ray diffraction data. McDaniel et al. (1983) also invoked this model to explain their results on dipalmitoylphosphatidylcholine bilayers suspended in highly concentrated glycerol and ethylene glycol solvents. On the basis of X-ray diffraction and differential scanning calorimetric studies, Serrallach et al. (1983) have reported an interdigitated gel phase for 1,3-dipalmitoylglycero-2-phosphocholine. In all of these recent studies, the acyl chains of various phospholipids are found to be interdigitated fully. That is, the acyl chain spans across the entire hydrocarbon width of the bilayer. Moreover, this fully interdigitated packing arrangement requires four hydrocarbon chains per lipid head group.

<sup>†</sup> From the Biophysics Department, Roswell Park Memorial Institute, Buffalo, New York 14263 (S.W.H.), and the Biochemistry Department, University of Virginia School of Medicine, Charlottesville, Virginia 22908 (J.T.M. and C.H.). Received January 6, 1984. This work was supported, in part, by Research Grants GM-17452 and GM-28120 from the National Institute of General Medical Sciences, NIH, U.S. Public Health Service.

We report here our X-ray diffraction and electron microscopic studies of the molecular packing of various asymmetric phosphatidylcholines with chain length differences from 1-stearoyl-2-caproyl-*sn*-glycero-3-phosphocholine [C(18):C(10)PC]<sup>1</sup> to C(18):C(18)PC. On the basis of results obtained in this work, we propose that, in the gel-state bilayer, highly asymmetric phosphatidylcholines such as C(18):C(10)PCs and C(18):C(12)PCs adopt a mixed interdigitated chain packing in which the long *sn*-1 acyl chain is interdigitated fully whereas the short *sn*-2 acyl chain packs end-to-end with another short *sn*-2 acyl chain of a different phospholipid molecule in the opposing bilayer leaflet. This mixed interdigitation demands three hydrocarbon chains per one lipid head group. The acyl chain packing of C(18):C(14)PCs in the gel-state bilayer, however, is distinctively different from that of the mixed interdigitated conformation. We propose that the C(18):C(14)PCs are packed in the gel-state bilayer with a highly disordered liquidlike region in the bilayer center, a structure similar to that exhibited by mitochondria lipids or egg phosphatidylcholines in the lamellar  $L_\beta$  phase (Tardieu et al., 1973).

### Materials and Methods

**Phospholipids.** C(18):C(10)PC, C(18):C(12)PC, and C(18):C(14)PC were all synthesized according to the established procedure developed in this laboratory (Mason et al., 1981). These mixed-chain phospholipids were better than 98 mol % pure with regard to the desired positional specificity of the fatty acids on the glycerol backbone. The chemical purity of the phosphatidylcholines was greater than 99 mol %. About 10 mg of the accurately weighed, dried, mixed-chain PCs were dispersed in given volumes of 50 mM KCl solution to produce a predetermined percentage of hydration. The exact percentage was checked by reweighing the sealed suspension. For samples containing excess water, the phospholipid suspensions were vortexed at a temperature above the phase transition temperature ( $T_m$ ) of the corresponding phospholipid (Mason et al., 1981). The dispersions were then concentrated by centrifugation at 3000g for 10 min. The loose pellets with abundant liquid content were taken for subsequent studies.

**X-ray Diffraction.** The samples were placed in the holding slot between two mica windows of an aluminum sample holder. The temperature of the sample holder was controlled to within  $\pm 0.5^\circ\text{C}$  of the set temperature. Fine-focus line source X-rays were generated in a Jarrell-Ash unit. Both wide-angle and small-angle diffraction patterns were recorded on film. The patterns were traced with a Joyce-Loebl Mark III densitometer. Detailed procedures were described previously (Hui & He, 1983).

All small-angle diffraction patterns revealed the presence of lamellar structures. From the lamellar repeat distance  $d$ , the concentration  $c$ , and the partial specific volume  $\bar{v}$  of the phospholipid in the sample, the bilayer thickness  $d_1$  can be derived by using the formula (Luzzati, 1968; Janiak et al., 1976)

$$d_1 = d[1 + \bar{v}_w(1 - c)/(c\bar{v})]^{-1} \quad (1)$$

where  $\bar{v}_w$  is the partial specific volume of water. For phospholipid suspensions, the value of  $c$ , measured in weight percent, is taken from the maximum hydration as determined

from swelling experiments (Janiak et al., 1976). Up to this water content,  $1 - c$ , a single, swelling lamellar phase exists, and above this maximum hydration a two-phase system composed of a fully swollen, lamellar phase and bulk water coexists. The partial specific volumes for various mixed-chain phosphatidylcholines are not known. Since C(18):C(10)PC and C(18):C(12)PC dispersions are found from Raman spectroscopic measurements to be highly ordered in the gel state (Huang et al., 1983), we assign a value of 0.93 mL/g as the mean partial specific volume for these two mixed-chain phospholipids. This value (0.93) corresponds to the lowest limiting value of  $\bar{v}$  for C(16):C(16)PC dispersions observed in the  $L_\beta'$  gel phase (Nagle & Wilkinson, 1982). On the other hand, C(18):C(14)PC dispersions display relatively disordered Raman spectra in both the 1000–1200- and the 2800–3100- $\text{cm}^{-1}$  regions in comparison with C(18):C(10)PC and C(18):C(12)PC dispersions (Huang et al., 1983). We assign a value of 0.98 mL/g as the mean partial specific volume for C(18):C(14)PC dispersions. The value of 0.98 corresponds to the measured  $\bar{v}$  for C(16):C(16)PC dispersions at  $T_m$  (Nagle & Wilkinson, 1978).

**Electron Microscopy.** Both negative-staining and freeze-fracture methods were used to study the morphology of phospholipid dispersions in excess aqueous solution. Negative-stained specimens were used to monitor vesicle size and the number of lamellae. In negative-staining experiments, the samples, microscope grids, and staining solution (2% ammonium molybdate) were equilibrated at given temperatures for at least 30 min. The sample was placed on the Formvar-carbon-coated grids previously rendered hydrophilic by glow discharge or by bacitracin treatment. The sample loading, staining, and air drying were all carried out at set temperatures. The dried grids were then examined in a Siemens 101 electron microscope.

Freeze-fracture samples were preequilibrated at given temperatures before being freeze quenched in liquid propane without cryoprotectant. The rapid freezing method using the sandwich technique (Costello & Coreless, 1978) and the environmental chamber employed have been described previously (Boni & Hui, 1983). Freeze-fracture was performed in a Polaron E7500 unit at  $-110^\circ\text{C}$  under ultrahigh vacuum as previously reported (Boni & Hui, 1983).

### Results

**Lamellar Repeat Spacings.** All lipids tested, including C(18):C(10)PC, C(18):C(12)PC, C(18):C(14)PC, C(16):C(16)PC, and C(14):C(14)PC, give one-dimensional crystalline diffractions in the small-angle region. The spacing ratio of 1:2:3:... suggests that these samples are multilamellar (Figure 1). The lamellar repeat spacings,  $d$ , of fully hydrated C(16):C(16)PC and C(14):C(14)PC at all experimental temperatures (10–45  $^\circ\text{C}$ ) agree with those reported by Janiak et al. (1976). The  $d$  values of the fully hydrated C(18):C(10)PC, C(18):C(12)PC, and C(18):C(14)PC at various temperatures are given in Figure 2. All these mixed-chain lipids show a significant increase in lamellar repeat spacing at their respective transition temperatures,  $T_m$ . The main-phase transition temperatures for C(18):C(10)PC, C(18):C(12)PC, and C(18):C(14)PC dispersions are 20, 18.5, and 30  $^\circ\text{C}$ , respectively (Mason et al., 1981). For C(18):C(12)PC and C(18):C(10)PC,  $d$  values decrease only gradually as the temperature increases above  $T_m$ . In the case of C(18):C(14)PC, the increase in  $d$  near  $T_m$  is dramatic (from 65 Å at 10  $^\circ\text{C}$  to 90 Å at 30  $^\circ\text{C}$ ), and the decrease in  $d$  above  $T_m$  is also rather steep. In spite of the one long stearic chain, the  $d$  values of C(18):C(10)PC and C(18):C(12)PC at  $T < T_m$  are con-

<sup>1</sup> Abbreviations: C(18):C(10)PC, 1-stearoyl-2-caproyl-*sn*-glycero-3-phosphocholine; C(18):C(12)PC, 1-stearoyl-2-lauroyl-*sn*-glycero-3-phosphocholine; C(18):C(14)PC, 1-stearoyl-2-myristoyl-*sn*-glycero-3-phosphocholine; C(10):C(10)PC, 1,2-dicaproyl-*sn*-glycero-3-phosphocholine; C(14):C(14)PC, 1,2-dimyristoyl-*sn*-glycero-3-phosphocholine; C(16):C(16)PC, 1,2-dipalmitoyl-*sn*-glycero-3-phosphocholine; C(18):C(18)PC, 1,2-distearoyl-*sn*-glycero-3-phosphocholine.

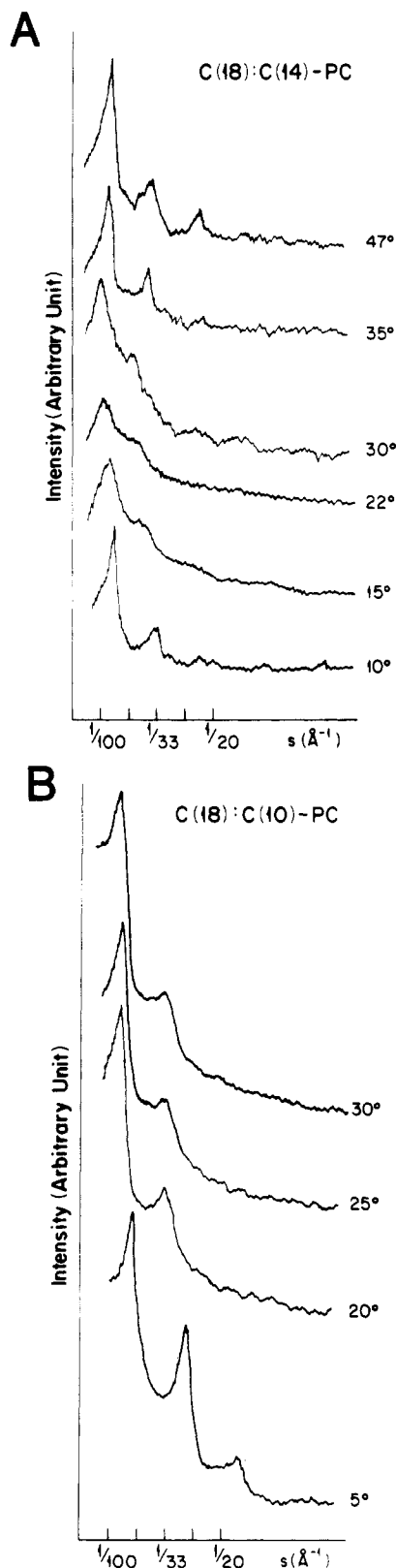


FIGURE 1: Intensity tracings of X-ray diffraction patterns from (A) fully hydrated C(18):C(14)PCs and (B) fully hydrated C(18):C(10)PCs at various temperatures.

siderably lower than those of C(16):C(16)PC and C(14):C(14)PC. For instance, the value of  $d$  at 10 °C for the first two lipids are respectively 54 and 55 Å, while those for the latter two lipids are respectively 63 and 61 Å.

**Bilayer Thickness Measurements.** In order to determine the value of  $d_1$  in excess water, swelling experiments were carried out for all unequal mixed-chain lipids at various tem-

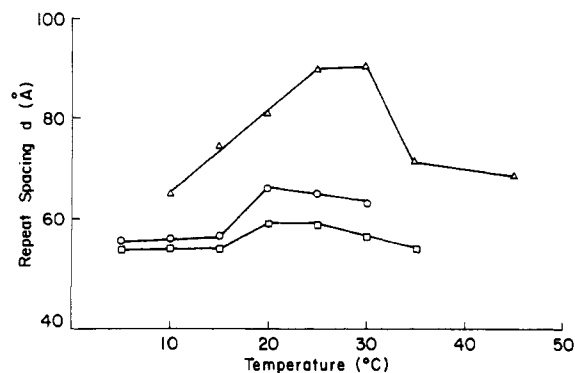


FIGURE 2: Temperature dependence of lamellar repeat spacings  $d$  of C(18):C(14)PC ( $\Delta$ ), C(18):C(12)PC ( $\circ$ ), and C(18):C(10)PC ( $\square$ ) dispersions.

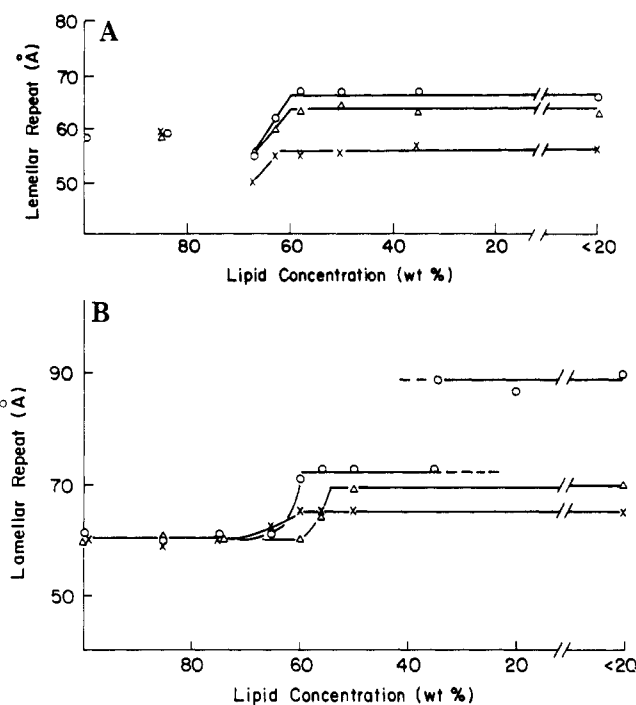


FIGURE 3: Hydration dependence of the lamellar repeat spacing of the following: (A) C(18):C(12)PC dispersions at 10 ( $\times$ ), 20 ( $\circ$ ), and 30 °C ( $\Delta$ ); (B) C(18):C(14)PC dispersion at 10 ( $\times$ ), 25 ( $\circ$ ), and 40 °C ( $\Delta$ ).

peratures. The maximum hydrations of these phospholipids were determined at temperatures above, at, and below their respective transition temperatures. The bilayer thickness was then calculated from eq 1.

The swelling results of C(18):C(10)PC and C(18):C(12)PC lamellae were similar. Both phospholipids attain a maximum hydration at a water content of 37% at 10 °C and 40% at 20 and 30 °C. The swelling curves of C(18):C(12)PC are shown in Figure 3A. These maximum hydration values are higher than those reported for C(14):C(14)PC at the corresponding temperatures (between 30% and 40%). The values of bilayer thickness,  $d_1$ , calculated for these phospholipid lamellae are plotted as a function of temperature in Figure 5. The value of  $d_1$  for C(14):C(14)PC bilayers measured by Janiak et al. (1976) is also included in Figure 5 for comparison. Apparently, at  $T < T_m$ , the bilayer thicknesses of both C(18):C(12)PC and C(18):C(10)PC lamellae are considerably less than that of C(14):C(14)PC lamellae. However, at  $T > T_m$ , the values of  $d_1$  of these highly asymmetric mixed-chain phospholipids are comparable to that of C(14):C(14)PC lamellae.

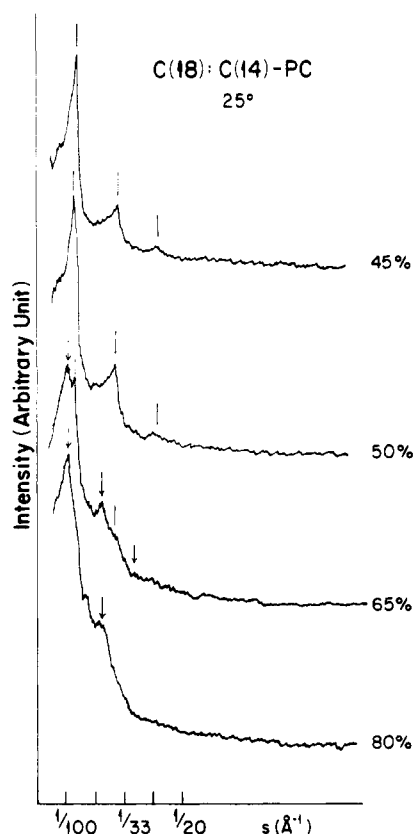


FIGURE 4: Intensity tracings of X-ray diffraction patterns from C(18):C(14)PCs in various degrees of hydration at 25 °C.

The swelling characteristics of C(18):C(14)PC are again different from the other two highly asymmetric mixed-chain phospholipids. Figure 3B shows the result of swelling studies on C(18):C(14)PC. The maximum hydration at 10 and 40 °C occurs at 40% and 45%, respectively. These maximal  $d$  values remain throughout all higher water content. At 25 °C, a temperature between  $T_m$  and the pretransition temperature, the  $d$  value reaches a plateau at a water content of 40% hydration. Immediately above this hydration, the value of  $d$  is 72 Å as indicated by the vertical bar in Figure 4. This value gives a bilayer thickness of 43 Å. At a water content of 65%, a second lamellar spacing of 90 Å can also be observed as shown by the arrow in Figure 4. Upon further swelling, this wider spacing becomes the sole repeat spacing (Figure 4). This value was used in Figure 2. On the basis of the assumption that the bilayer thickness remains unchanged through the swelling process, the drastic increase in  $d$  is again attributable to another step of increase in the water spacing between bilayers. The coexistence of two swelling states at 65% hydration indicates that the system is not yet in total equilibrium. Spacings in such a heterogeneous system cannot be used to calculate  $d_1$ . Therefore, the value of 43 Å is more reliable for  $d_1$  at 25 °C. The values of  $d_1$  for C(18):C(14)PCs as a function of temperature are also given in Figure 5. Below  $T_m$ , these values of  $d_1$  are slightly less than those of C(14):C(14)PC. At  $T > T_m$ , however, the  $d_1$  value of C(18):C(14)PC is consistently higher than that of C(14):C(14)PC.

**Wide-Angle X-ray Diffraction.** At  $T > T_m$ , wide-angle diffractions of fully hydrated C(18):C(10)PC, C(18):C(12)PC, and C(18):C(14)PC lamellae all show a barely detectable diffuse reflection at 4.6 Å. At  $T < T_m$ , C(18):C(14)PC lamellae give a sharp reflection at 4.2 Å, typical of phospholipids in the gel state. The line shape of the reflection at 4.2 Å is radially symmetrical (Figure 6a), indicating that the tilt angle of the phospholipid acyl chains with respect to the bilayer

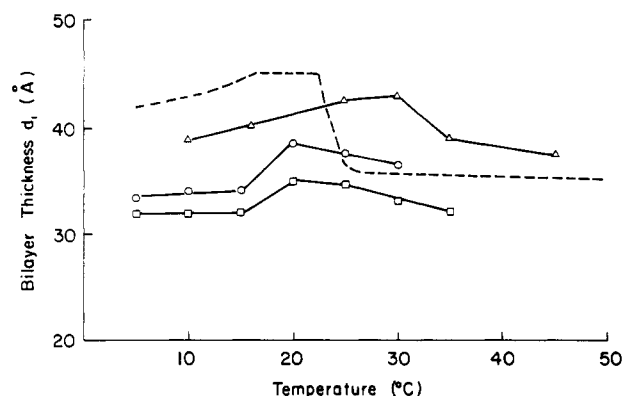


FIGURE 5: Temperature dependence of the calculated bilayer thickness,  $d_1$ , of C(18):C(14)PC ( $\Delta$ ), C(18):C(12)PC (O), and C(18):C(10)PC ( $\square$ ) dispersions. The bilayer thickness of C(14):C(14)PC dispersion calculated by Janiak et al. (1976) is drawn in as (---) for comparison.

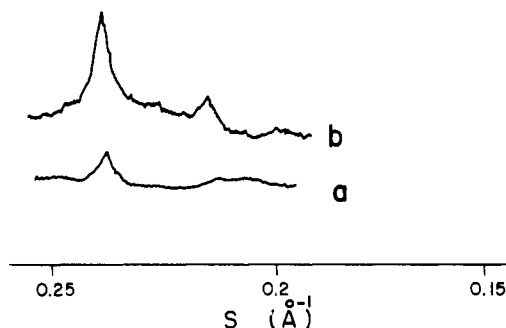


FIGURE 6: Intensity tracings of the wide-angle, X-ray diffraction of (A) C(18):C(14)PC and (B) C(18):C(10)PC, both at 10 °C.

normal is not significant (Tadieu et al., 1973; Janiak et al., 1976; Hui, 1976). Both C(18):C(10)PC and C(18):C(12)PC samples show another weaker but sharp line at  $d = 4.6$  Å (Figure 6b) at  $T < T_m$ . The additional reflection line indicates that the hexagonal packing commonly seen in gel-state phospholipids no longer holds. When these highly asymmetric mixed-chain phospholipids, C(18):C(10)PC and C(18):C(12)PC samples, are left standing for 5 days or more at  $T < T_m$ , or partially dehydrated, often an additional pair of lines at  $d = 4.8$  and 5.0 Å are detectable. These additional high-angle lines show that these highly asymmetric mixed-chain phospholipids become increasingly crystalline upon storage even in a fully hydrated state. Identification of the space group of the acyl chain packing based on a few "powder" diffraction lines is not justified.

**Electron Microscopy.** In view of the unusual findings by X-ray diffraction, both negative-staining and freeze-fracture electron microscopy methods were used to obtain more insight into these structures. The morphology of C(18):C(10)PC and C(18):C(12)PC suspensions in excess water is similar. Both phospholipids form a mixture of large multilamellar liposomes and smaller (600 Å) vesicles. A feature distinguishing these highly asymmetric mixed-chain phospholipids from the equal chain ones is that at  $T < T_m$ , the freeze-fracture faces of the former are discontinuous. Instead of fracturing along the bilayer interior, the fracture planes are often interrupted by up or down steps as if there is no preferred fracture plane of weakest bonding (Figure 7A). At  $T > T_m$ , the fracture planes are more continuous, although disrupted patterns are occasionally seen. There appear to be more smaller vesicles at  $T > T_m$ . The size and the number of lamellae of the larger liposomes are not as large as those of multilamellar liposomes of equal chain-length phospholipids. This size difference was also noted by Mason et al. (1983).

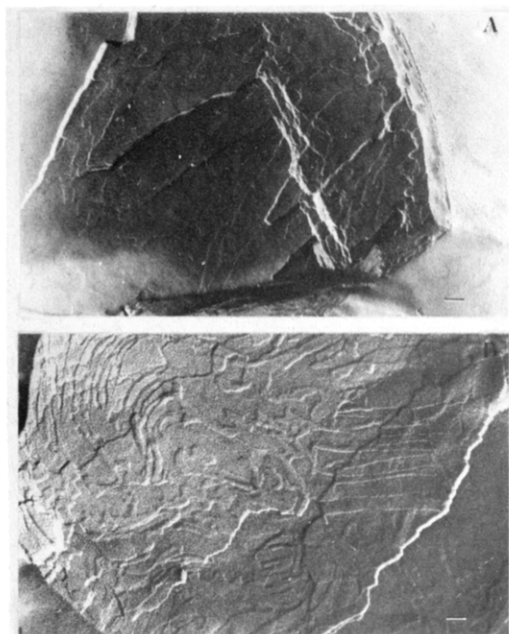


FIGURE 7: Freeze-fracture electron micrographs of (A) C(18):C(10)PC at 5 °C and (B) C(18):C(14)PC at 10 °C. Bar = 0.1  $\mu$ m.

The morphology of C(18):C(14)PC dispersions detected by freeze-fracture electron microscopy is quite different from the other two highly asymmetric mixed-chain phospholipid dispersions just discussed. At 10 °C, the fracture face shows a terrace and banded pattern (Figure 7B) as seen in many phospholipid liposomes (Stewart et al., 1979). At 25 °C, a temperature between the thermal pretransition and main transition of C(18):C(14)PC, the freeze-fracture morphology is definitely a  $P_\beta$ -type structure (Figure 8). In many liposomes, the lamellae are clearly seen to be widely separated by a water space (Figure 8A); moreover, smaller vesicles are often present between this wide interlamellar gap (Figure 8A,B). Many multilamellar liposomes are seen to be broken into a collection of small vesicles (Figure 8B). Smaller vesicles "budding" from lamellae, as well as suggestive contact markers of small vesicles on the lamellae (Figure 8C), are often observed. At  $T > T_m$ , the samples are dominated by smaller vesicles. The fracture faces on the remaining large multilamellar liposomes show a "jumbled" pattern which is thought to be the remnant of the  $P_\beta$  structure (Stewart et al., 1979; Luna & McConnell, 1978). The size change through the phase transition is also evident from negative-stain images (Figure 9).

#### Discussion

One of the most interesting results obtained in this study is the observation that the bilayer thickness of C(18):C(10)PCs and C(18):C(12)PCs in the bilayer gel state is considerably lower than the corresponding value for C(14):C(14)PC lamellae (Figure 5). It should be pointed out, however, that the bilayer thickness of C(18):C(10)PC and C(18):C(12)PC lamellae was calculated on the basis of the assumed value of partial specific volume (0.93 mL/g). It is well-known that the partial specific volume of phosphatidylcholines is relatively insensitive to temperature. The largest change in  $\bar{v}$  for synthetic phosphatidylcholines occurs at the gel  $\rightarrow$  liquid-crystalline phase transition, and the overall relative change in  $\bar{v}$  across the phase transition temperature is merely 3.7% for C(16):C(16)PC dispersions (Nagel & Wilkinson, 1978). If the value of 0.93 mL/g is taken to have a maximum error of 3.7%, it will only affect the calculated bilayer thickness by 1

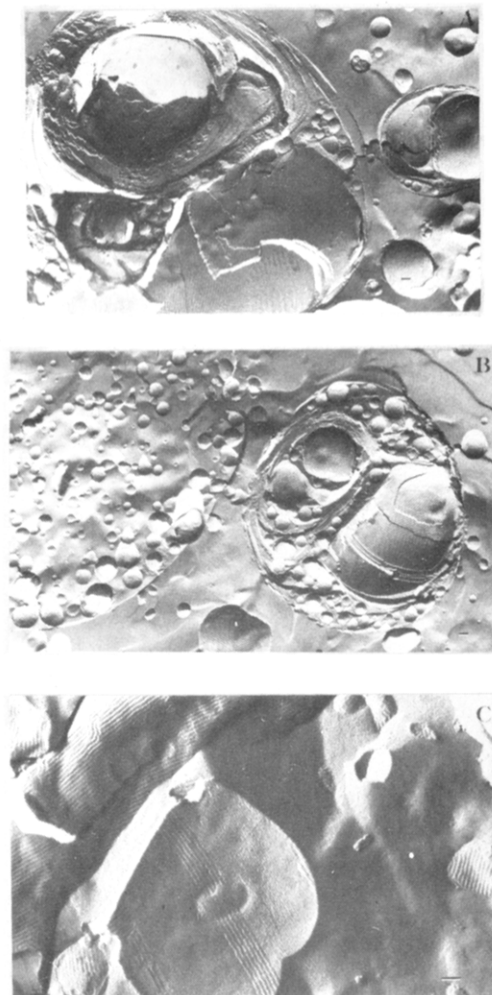


FIGURE 8: Freeze-fracture electron micrographs of C(18):C(14)PC (A, B) at 25 and (C) 30 °C.



FIGURE 9: Negative-stain electron micrograph of C(18):C(14)PC at 27 °C.

$\text{\AA}$ , which is certainly within the experimental error of our X-ray diffraction measurements. Clearly, any reasonable error in  $\bar{v}$  cannot possibly explain the observed large difference (10  $\text{\AA}$ ) in the bilayer thickness between C(18):C(10)PC and C(14):C(14)PC lamellae at 10 °C (Figure 5).

Since the total number of methylene units in the hydrocarbon core of bilayers composed of C(18):C(10)PCs and C(14):C(14)PCs is identical, one might expect that if the mixed-chain C(18):C(10)PCs form bilayers with both the acyl chains of the opposing monolayers interdigitated as shown in Figure 10A, the bilayer thickness would be identical with that of the C(14):C(14)PC lamella. In light of the new X-ray result that the gel-state bilayer thickness of C(18):C(10)PC lamellae is approximately 10  $\text{\AA}$  smaller than that of C(14):C(14)PC lamellae, the packing model first presented by Mason et al.

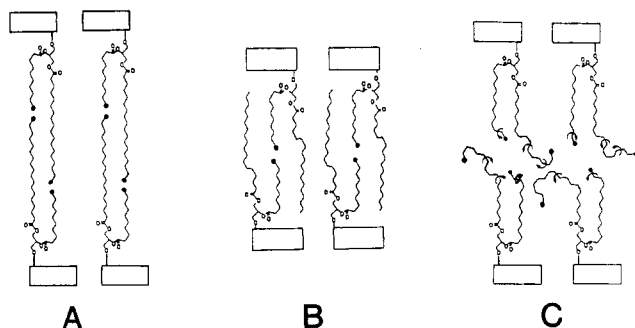


FIGURE 10: Possible acyl chain packing models for the C(18):C(10)PC gel-state bilayers: (A) The interdigitated model proposed by Mason et al. (1981). (B) The mixed interdigitated model suggested by this work. A schematic representation of the proposed C(18):C(14)PC gel-state bilayer (C) is characterized by a liquidlike thin layer of hydrocarbon chain terminals sandwiched by relatively ordered chain segments oriented perpendicular to the lamellar surface.

(1981) as shown in Figure 10A must be modified.

One possible explanation for the shorter bilayer thickness could be attributed to tilting of the hydrocarbon chains of the phosphatidylcholines. In order to shorten the bilayer thickness from 43 to 33 Å, the acyl chains would have to be tilted with respect to the bilayer normal by an angle of 39.9°. Such a tilt angle would produce a definite asymmetry in the wide-angle reflection at 4.2 Å (Tadieu et al., 1973; Janiak et al., 1976). The symmetrical shape and sharpness of the 4.2-Å diffraction line in the wide-angle region (Figure 6) suggest that the hydrocarbon chains of C(18):C(10)PCs are essentially untilted with respect to the bilayer normal.

Alternatively, one can postulate that the *sn*-1 acyl chains of the C(18):C(10)PCs in the gel-state bilayer are folded back to fill the void volume beneath the shorter *sn*-2 acyl chains. Because of the bend, the bilayer is thinner than for C(14):C(14)PC. In this model, the acyl chains in the two leaflets are noninterdigitated. Furthermore, the linear chain segments that are in contact with the neighboring methyl groups must be perturbed by the bulky methyl groups, thereby causing *trans* → *gauche* isomerizations of the C—C bonds. The situation is similar to the complementary packing suggested between the phospholipid acyl chain and the  $\beta$ -surface of cholesterol molecules having two puckered angular methyl groups (Huang, 1977). In addition, more *gauche* bonds must be converted from the C—C *trans* bonds near the center of the bilayer so that the *sn*-1 acyl chain can be folded back to fill the void space beneath the *sn*-2 chain. Clearly, one would expect relatively larger *gauche*/*trans* ratios for C(18):C(10)PC bilayers in comparison to C(18):C(18)PC bilayers. Results obtained from Raman studies of the mixed-chain PCs clearly ruled out this possibility, because both the interchain and intrachain order/disorder parameters for C(18):C(10)PC and C(18):C(18)PC bilayers are virtually identical at the same reduced temperature in the gel state (Huang et al., 1983).

A model which can best explain both the shorter bilayer thickness and the highly ordered bilayer structure of C(18):C(10)PCs is presented in Figure 10B. Specifically, the shorter *sn*-2 acyl chain of the asymmetric mixed-chain phospholipid molecules in the gel state is proposed to pack end-to-end with the *sn*-2 acyl chain of another lipid molecule in the opposing bilayer leaflet, while the longer *sn*-1 acyl chain from the two leaflets adopts a totally interdigitated conformation similar to that exhibited by dipalmitoylphosphatidylglycerol in the presence of choline or acetylcholine (Ranck & Tocanne, 1982), dipalmitoylphosphatidylcholine in the presence of glycerol or ethylene glycol (McDaniel et al., 1983), and 1,3-dipalmitoylglycero-2-phosphocholine in the

$L_{\beta}^i$  phase (Serrallach et al., 1983).

On the basis of the proposed model, the sum of two C(10) *sn*-2 acyl chains should match nearly perfectly in length with the longer C(18) *sn*-1 acyl chain in the gel-state bilayer (Figure 10B). Since the volume of the acyl chain terminal methyl group is bulkier than that of the acyl chain methylene group, the *sn*-1 acyl chain segment adjacent to the *sn*-2 methyl groups is most likely to undergo some degrees of conformational change, such as *trans* → *gauche* isomerizations, to complement laterally the slightly bulkier methyl groups as shown in Figure 10B, thus shortening the *sn*-1 acyl chain somewhat. Nevertheless, the C(18):C(10)PC lamella in the gel state, according to Figure 10B, can be expected to have a bilayer thickness more or less equivalent to the value for noninterdigitated C(10):C(10)PC bilayers. Experimental data obtained with C(10):C(10)PC lamellae indeed bear this out. The bilayer thicknesses determined at -8 and 0 °C for C(10):C(10)PC lamellae are 31 and 34 Å, respectively, which are in excellent agreement with the value of 33 Å for C(18):C(10)PC lamellae determined at 10 °C.

Support for the proposed mixed interdigitated model in which the *sn*-1 acyl chain is fully interdigitated whereas the *sn*-2 acyl chain is noninterdigitated is also obtained from the calculation of the average area available to one C(18):C(10)PC molecule at the bilayer-H<sub>2</sub>O interface at 10 °C. The average area ( $A$ ) can be calculated to be 63 Å<sup>2</sup> according to the equation  $A = 2M\bar{v}/(d_1N) \times 10^{-24}$  where  $M$  is the molecular weight of the phospholipid molecule (678 g·mol<sup>-1</sup>),  $d_1$  is the bilayer thickness (33 Å),  $\bar{v}$  is the partial specific volume of the lipid (0.93 mL·g<sup>-1</sup> at 10 °C), and  $N$  is Avogadro's number. Since the cross-sectional area of one all-*trans* phospholipid acyl chain in the lamellar phase is  $\Sigma = 20.4$  Å<sup>2</sup> (Luzzati, 1968), the ratio of  $A/\Sigma$  is approximately 3, a value required for the proposed packing model shown in Figure 10B.

The bilayer structure of C(18):C(12)PCs in the gel state is suggested to be similar to the one proposed for C(18):C(10)PCs (Figure 10B), except that kinks near the CH<sub>3</sub> ends of *sn*-2 chains are most likely present in the mixed interdigitated bilayer. The presence of kinks will not significantly perturb the lateral chain packing but will shorten the bilayer thickness (Lagaley & Weiss, 1971; Lagaley, 1976). The small difference in the gel state bilayer thickness between C(18):C(10)PCs and C(18):C(12)PCs as demonstrated in Figure 5 can probably be attributed to the possible presence of kinks near the bilayer center. Kinks similar to the ones discussed here have been detected recently in the highly ordered phase of solid *n*-alkanes (Maroncelli et al., 1982).

At  $T < T_m$  the wide-angle diffraction patterns of the dispersions of C(18):C(10)PC and C(18):C(12)PC indicate that their chain packing is not hexagonal. If the *sn*-1 and *sn*-2 acyl chains are not equivalent, as in the case of highly asymmetric mixed-chain phospholipids, the hexagonal packing symmetry no longer exists. A simple model that places the *sn*-1 and *sn*-2 acyl chains in alternating rows yields instead a tetragonal or an orthorhombic lattice. If the 4.2- and 4.6-Å lines are assumed to be the (020) and the (110) reflection of an orthorhombic lattice, respectively, then the lattice constants can be calculated to be  $a = 5.5$  Å and  $b = 8.4$  Å.

A nonhexagonal type of diffraction was also observed in the cochleate form of phosphatidylserine-calcium complex (Jacobson & Papahadjopoulos, 1975; Hui et al., 1983) and was interpreted as the acyl chains being locked in an orthorhombic lattice (Newton et al., 1978). Saturated and equal chain phosphatidylcholines, phosphatidylethanolamines, phosphatidylglycerols, galactosylglycerols, and sphingolipids are all



known to have a form of higher crystallinity which gives nonhexagonal diffraction patterns (Ruoco et al., 1981; Harlos, 1978; Harlos & Eibl, 1980a,b; Curatolo et al., 1982; Ruoco et al., 1982; Sen et al., 1983). This highly ordered phase implies that the spatial orientations of the lipid molecules in the bilayer are specified through the interlocking of inequivalent acyl chains or hydrogen or cation bonding between adjacent head groups (Ruoco et al., 1981). In the case of  $L_c$  phase, the formation of this higher order nonhexagonal type phase usually requires prolonged annealing and is dependent on dehydration (Ruoco et al., 1982; Harlos & Eibl, 1980b; Chang & Epand, 1983; Sen et al., 1983). The commonly known "gel" phase with hexagonally packed acyl chains is thus referred to as an intermediate "metastable" state. Our C(18):C(10)PC and C(18):C(12)PC samples, however, form the highly ordered phase readily upon cooling in excess water, indicating that forces additional to hydrogen bonding are acting in favor of the formation of a highly crystalline state. It is reasonable to suppose that at temperatures considerably below  $T_m$  chain interdigitation goes hand in hand with the formation of a highly ordered crystalline state within which chain positions are not interchangeable.

The structural characteristics of C(18):C(14)PC dispersions are quite different from the other two highly asymmetric mixed-chain phospholipid dispersions just discussed. The bilayer thickness in the gel state is disproportionally higher than those of the other two. Moreover, it displays a  $P_\beta$  phase (Figure 8A) at temperatures between the pretransition (19 °C) and the main-phase transition temperature (30 °C).

Before we discuss our X-ray diffraction data obtained from C(18):C(14)PC lamellae, it is pertinent to consider our Raman spectroscopic studies which indicate that the C(18):C(14)PC lamella at the gel state exhibits the highest inter- and intrachain conformational disorder among dispersions of C(18):C(10)PC, C(18):C(12)PC, C(18):C(14)PC, C(18):C(16)PC, and C(18):C(18)PC (Huang et al., 1983). We have discussed the mixed interdigitated bilayer structure of C(18):C(12)PCs in terms of the formation of kinks in the region near the  $\text{CH}_3$  ends of *sn*-2 acyl chains. Since the C(18):C(14)PC bilayer is conformationally more disordered than the C(18):C(12)PC bilayer in terms of both the intrachain and interchain packing, the formation of additional kinks in the *sn*-1 and *sn*-2 acyl chains for C(18):C(14)PC lamellae must be inferred if both the C(18):C(14)PCs and C(18):C(12)PCs form the same type of mixed interdigitated bilayer structure.

If one introduces additional kinks into both of the acyl chains of the C(18):C(14)PC molecule, it becomes evident that the length of the C(18) *sn*-1 acyl chain is less than sufficient to match laterally with the sum of two C(14) *sn*-2 acyl chains in the bilayer structure as is shown in Figure 10B. One is led to conclude that the mixed interdigitated model proposed for the gel-state bilayer of C(18):C(10)PC and C(18):C(12)PC should not be applied to the bilayer structure of C(18):C(14)PC. Instead, we suggest that the C(18):C(14)PCs are packed in the gel-state bilayer with the chain conformations similar to those exhibited by mitochondria lipids or egg phosphatidylcholines in the lamellar  $L_\beta$  phase (Tardieu et al., 1973). Basically, the chain segments containing the first 10 or 11 methylene units are packed with rotational disorder in a two-dimensional hexagonal lattice, and they are oriented at right angles to the bilayer surface; these are characterized by the only symmetrical 4.2-Å reflection in the wide-angle region (Figure 6a). Due to a difference in chain length between the *sn*-1 and *sn*-2 acyl chains and the dynamic nature of the short-chain segment at the  $\text{CH}_3$  ends, a precise chain-chain

van der Waals contact is thus not possible beyond the C(11) atom along the *sn*-2 acyl chain. This leads to a highly disordered liquid-like region in the center of the C(18):C(14)PC bilayer (Figure 10C).

At  $T > T_m$ , the bilayer thicknesses of C(18):C(12)PC and C(18):C(10)PC lamellae are comparable to that of the C(14):C(14)PC bilayer, which represents the average chain length of the phospholipids we studied. The same holds for C(18):C(14)PC bilayer as compared to C(16):C(16)PC bilayer. The results support the view that at  $T > T_m$  the acyl chains are highly dynamic and may not interdigitate significantly. Consequently, the bilayer thickness can be approximated to the average chain length of the two unequal chains.

The proposed mixed-chain interdigitation in multilamellar bilayers of C(18):C(10)PCs and C(18):C(12)PCs in the gel state is further supported by the fact that, at  $T < T_m$ , the freeze-fracture plane of these phospholipids is irregular. The fact that all the methyl terminals are not coplanar prevents a smooth fracture face, which is expected for membranes with a smooth, weak bonding plane in the center of the noninterdigitated bilayer. On the other hand, freeze-fracture studies of C(18):C(14)PC lamellae have revealed smooth and continuous fracture planes; this is consistent with the proposed model presented in Figure 10C in which a thin liquidlike hydrocarbon region is presumably present in the bilayer center of C(18):C(14)PC lamellae in the gel state.

It is interesting to note that, during the pretransition, many large multilamellar C(18):C(14)PC structures are observed breaking into smaller vesicles (Figure 8A,B and Figure 9). It is possible that, above the pretransition temperature, the inequivalent methyl ends of the C(18) *sn*-1 and C(14) *sn*-2 acyl chains in the bilayer can be matched more evenly as caused partly by the formation of the  $P_\beta$  structure (Sackman, 1983) and partly by the high radius of curvature for the small vesicles. This molecular packing rearrangement in the C(18):C(14)PC bilayer induced by the endothermic pretransition leads to a different hydration requirement for the head group, resulting in a larger interlamellar water spacing (Figure 2) as well as the formation of numerous small vesicles. The process of lamellar swelling and small vesicle formation can be readily seen from freeze-fracture replicas of C(18):C(14)PC dispersions which have been incubated at 25 °C prior to rapid freezing (Figure 8A,B). Since the endothermic phase transition involves vesicle size alteration, and since the change in vesicle size discernibly affects the thermal properties of the lipid dispersion (Mason et al., 1983), we therefore expect that the calorimetric behavior of these lipid dispersions is not strictly reversible or at least involves some degree of hysteresis. This is in fact shown to be the case (Mason et al., 1981; unpublished results). The dependence of the calorimetric behavior of these lipid dispersions on their thermal history, especially in the case of C(18):C(14)PC, can be attributed, at least in part, to the breakdown of large multilamellar structures into small vesicles at the lower phase transition temperature. Results of  $^{31}\text{P}$  NMR on C(18):C(14)PC dispersions at  $T > T_m$  also demonstrate a preponderance of very small vesicles which result in a substantial narrowing of the  $^{31}\text{P}$  NMR spectra for this lipid (unpublished results). This fact adds more complications to the interpretation of the calorimetric results. One should, therefore, be extremely cautious when attempting to explain the thermal behavior of asymmetric mixed-chain lipids isolated from biological membranes such as sphingolipids or glycosphingolipids; in fact, large multilamellar structures of sphingomyelin have indeed been observed to shatter into many small vesicles when they are heated above the phase transition

temperature (Hui et al., 1980). Needless to say, any in vivo investigation employing fluorescent lipid analogues, in which the probe is covalently attached to the C(2) atom of the glycerol backbone and the overall length of the probe is distinctively different from that of the *sn*-2 acyl chain normally found in the major phospholipid of biomembranes, should not consider the analogue as a representative "normal" lipid species of biological membranes without justification, since these fluorescent lipid analogues may form mixed interdigitated lamellae with themselves or with other asymmetric lipid species in the biological membrane.

Since the submission of this paper, a X-ray diffraction study of fully hydrated C(18):C(10)PCs has been reported by McIntosh et al. (1984a). Subsequently, Dr. T. J. McIntosh kindly sent us a copy of their paper (McIntosh et al., 1984b) in which the electron density profile of C(18):C(10)PC dispersions is calculated. Their conclusion regarding the molecular packing of C(18):C(10)PCs in the gel-state bilayer is in good agreement with ours as described here.

#### Acknowledgments

The assistance of T. Isac, L. T. Boni, and N. B. He in various parts of data collection is greatly appreciated. C.H. gratefully acknowledges Lee Shih-ching for the timely encouragement before the resubmission of the manuscript for publication.

**Registry No.** C(18):C(10)PC, 78119-50-3; C(18):C(12)PC, 7276-39-3; C(18):C(14)PC, 20664-02-2; C(10):C(10)PC, 3436-44-0; C(14):C(14)PC, 18194-24-6; C(16):C(16)PC, 63-89-8; C(18):C(18)PC, 816-94-4.

#### References

- Boggs, J. M., Stamp, D., & Moscarello, M. A. (1981) *Biochemistry* 20, 6066-6072.
- Boni, L. T., & Hui, S. W. (1983) *Biochim. Biophys. Acta* 731, 177-185.
- Chang, H., & Epand, R. M. (1983) *Biochim. Biophys. Acta* 728, 319-321.
- Chapman, D., Williams, R. M., & Ladbroke, B. D. (1967) *Chem. Phys. Lipid* 1, 445-475.
- Costello, M. J., & Corless, J. M. (1978) *J. Microsc.* 112, 17-26.
- Curatolo, W., Bali, A., & Gupta, C. M. (1982) *Biochim. Biophys. Acta* 690, 89-94.
- Harlos, K. (1978) *Biochim. Biophys. Acta* 511, 348-355.
- Harlos, K., & Eible, H. (1980a) *Biochemistry* 19, 895-899.
- Harlos, K., & Eible, H. (1980b) *Biochim. Biophys. Acta* 601, 113-122.
- Huang, C. (1977) *Lipids* 12, 348-356.
- Huang, C., & Levin, I. W. (1983) *J. Phys. Chem.* 87, 1509-1513.
- Huang, C., Lapidus, J. R., & Levin, I. W. (1982) *J. Am. Chem. Soc.* 104, 5926-5930.
- Huang, C., Mason, J. T., & Levin, I. W. (1983) *Biochemistry* 22, 2775-2780.
- Hui, S. W. (1976) *Chem. Phys. Lipids* 16, 9-18.
- Hui, S. W., & He, N. B. (1983) *Biochemistry* 22, 1159-1164.
- Hui, S. W., Stewart, T. P., & Yeagle, P. L. (1980) *Biochim. Biophys. Acta* 601, 271-281.
- Hui, S. W., Boni, L. T., Stewart, T. P., & Isac, T. (1983) *Biochemistry* 22, 3511-3516.
- Jacobson, K., & Papahadjopoulos, D. (1975) *Biochemistry* 14, 152-161.
- Janiak, M. J., Small, D. M., & Shipley, G. G. (1976) *Biochemistry* 15, 4575-4580.
- Lagaly, G. (1976) *Angew. Chem., Int. Ed. Engl.* 15, 575-586.
- Lagaly, G., & Weiss, A. (1971) *Angew. Chem., Int. Ed. Engl.* 10, 558-559.
- Luzzati, V. (1967) in *Biological Membranes* (Chapman, D., Ed.) Academic Press, New York.
- Maroncelli, M., Qi, S. P., Strauss, H. L., & Snyder, R. G. (1982) *J. Am. Chem. Soc.* 104, 6237-6247.
- Mason, J. T., & Huang, C. (1981) *Lipids* 16, 604-608.
- Mason, J. T., Huang, C., & Bittonen, R. L. (1981) *Biochemistry* 20, 6086-6092.
- Mason, J. T., Huang, C., & Bittonen, R. L. (1983) *Biochemistry* 22, 2013-2018.
- McDaniel, R. V., McIntosh, T. J., & Simon, S. A. (1983) *Biochim. Biophys. Acta* 731, 97-108.
- McIntosh, T. J., Simon, S. A., Ellington, J. C., Jr., & Porter, N. A. (1984a) *Biophys. J.* 45, 41a (Abstr. No. M-PM-D11).
- McIntosh, T. J., Simon, S. A., Ellington, J. C., Jr., & Porter, N. A. (1984b) *Biochemistry* 23, 4038-4044.
- Nagle, J. F., & Wilkinson, D. A. (1978) *Biophys. J.* 23, 159-175.
- Nagle, J. F., & Wilkinson, D. A. (1982) *Biochemistry* 21, 3821-3830.
- Newton, C., Pangborn, W., Nir, S., & Papahadjopoulos, D. (1978) *Biochim. Biophys. Acta* 506, 281-287.
- Pearson, R. H., & Pascher, I. (1979) *Nature (London)* 281, 499-501.
- Ranck, J. L., & Tocanne, J. F. (1982) *FEBS Lett.* 143, 171-174.
- Ranck, J. L., Keira, T., & Luzzati, V. (1977) *Biochim. Biophys. Acta* 488, 431-441.
- Ruocco, M. J., & Shipley, G. G. (1982) *Biochim. Biophys. Acta* 684, 59-66.
- Ruocco, M. J., Atkinson, D., Small, D. M., Skarjune, R. P., Oldfield, E., & Shipley, G. G. (1981) *Biochemistry* 20, 5957-5966.
- Sackman, E., Ruppel, D., & Gebhardt, C. (1980) in *Chemical Physics* (Helfrich, W., & Heppke, G., Ed.) Vol. II, Springer-Verlag, New York.
- Sen, A., Mannock, D. A., Collins, D. J., Quinn, P. J., & Williams, W. P. (1983) *Proc. Roy. Soc. B* 218, 349-364.
- Serrallach, E. N., Dijkman, R., de Haas, G. H., & Shipley, G. G. (1983) *J. Mol. Biol.* 170, 155-174.
- Stewart, T. P., Hui, S. W., Portis, A. R., & Papahadjopoulos, D. (1979) *Biochim. Biophys. Acta* 556, 1-16.
- Tadieu, A., Luzzati, V., & Reman, F. C. (1973) *J. Mol. Biol.* 75, 711-733.